METALLURGY AND FOUNDRY ENGINEERING – Vol. 38, 2012, No. 1
http://dx.doi.org/10.7494/mafe.2012.38.1.55

Paweł Leszek Żak*, Józef Szczepan Suchy**

NUMERICAL MODEL FOR DENDRITE GROWTH – AN APPLICATION OF THE RANK CONTROLLED DIFFERENTIAL QUADRATURE METHOD

1. INTRODUCTION

Increasing demand for high quality products and tendency to production costs reduction impose the use of innovative and advanced modelling techniques. Competition between companies causes use of basic modelling tools being insufficient. That is why computer intended algorithms more often take into account processes that run at micro- and even nano- scale. For those processes only the application of more sophisticated numerical methods can lead accurate solutions.

Numerical modelling and computer simulation can lead to casting technology optimization in the sense of production cost reduction [1, 2]. Mathematical methods and models can be very helpful during developing modern methods of experimental data examination [3].

In this paper the authors attempt to build a numerical model that could help determine a mutual relationship between the concentration field on an axis that joins the centre of the dendrite with its tip and the dendrite growth rate. Within this work, the algorithm for solving the mathematical model published by Żak *et al*. [4] was developed. The numerical model was created on the base of the RCDQ approximation of spatial derivatives that appears in PDEs. The introduced model can be used to predict dendrite growth rate in alloy. The prepared numerical model can be useful even in the case of compound alloys while it is possible to reduce compound alloys to binary according to the additivity rule [5].

Attempts to develop such mathematical models have been taken by various authors [6–8]. However, the numerical method used in this work is innovative. The Rank Controlled Diffe-rential Quadrature method is a modification of the Differential Quadrature (DQ) method that was first developed by Bellman [9, 10].

* M.Sc., **Prof., Ph.D., D.Sc.: AGH University of Science and Technology, Faculty of Foundry Engineering, Krakow, Poland, e-mail: pawelzak@agh.edu.pl

DQ definition

The f function defined in $[a, b]$ interval is considered, a set of N discrete coordinates x_i:

$$S = \{x_i : a = x_1 < x_2 < ... < x_N = b\} \tag{1}$$

is the grid introduced in the computational domain. The DQ is a method for a spatial partial derivative of unknown field function f approximation as a linear weighted sum of the function values at grid points:

$$\frac{\partial^n f}{\partial x^n}(x_i) = \sum_{j=1}^{N} \omega_{i,j}^{(n)} f(x_j) \tag{2}$$

where: $\frac{\partial^n f}{\partial x^n}(x_i)$ denotes the nth derivative of the function f with respect to x in point x_i; $\omega_{i,j}^{(n)}$ are the quadrature weighting coefficients and $f(x_j)$ are the function values at the x_j.

DQ was applied in numerous physical problems, since explicit method for weighting coefficient calculations was proven by Quan and Chang [11, 12]. The rank of DQ method depends on the grid points number, N, and is equal to $(N-n)$ [13]. Especially, for dense grids this feature can cause problems. The first problem is the computational effort. As the grid gets thicker more multiplications and summations must be made to obtain the approximate value of the function derivative in the next time step (Eq. 2). The relationship between the interpolation and the DQ can be shown [14]. This causes Lebesgue constant influence on method accuracy. This is the parameter that depends on grid point numbers and their distribution. It was shown by Vertesi [15] minimal Lebesgue constant for optimal grid is asymptotically equal to $\frac{2}{\pi}\log(N+1) + \frac{2}{\pi}(0.577215... + \log\frac{4}{\pi}) + o\left((\frac{\log\log N}{\log N})^2\right)$, where o denotes Landau symbol. An estimation for the Lebesgue constant for uniform grid is even greater [16]. This fact gives information that if the grid gets more dense the error also grows. After a specific value of N, the error that comes from the Lebesgue constant is some order of magnitude greater than this that can be reduced by improving method rank.

To avoid the problems mentioned above the authors introduced a modification of DQ named Rank Controlled Differential Quadrature [14, 17]. This methods based on an idea of reduced calculation domain grid points number to obtain a specific rank of quadrature during the calculation of derivation approximate value. Rank of the approximation should be chosen in the way that assure good accuracy, but not too high, to avoid the growing of Lebesgue constant problem. This approach lets reduce the computational effort, as for dense grids most of the weighting coefficients would be equal to zero (in computational practice those multiplications can be omitted).

2. THE NUMERIC METHOD

The Rank Controlled Differential Quadrature method is the modification of the DQ method. Improving the DQ leads to increased computation accuracy, lowering the computational effort and overcoming the high Lebesgue constant problem. In this method the partial derivative of unknown field function f is approximated as a linear weighted sum of the function values at specified grid points:

$$\frac{\partial^n f}{\partial x^n}(x_i) = \sum_{j=S1(i)}^{j=S2(i)} \omega_{i,j}^{(n)} f(x_j) \tag{3}$$

For each point, i, of the grid S (Eq. 1) the rank distribution representation is defined, $R_{DQ}(i)$. With this function the limitations for grid points indices $S1$, $S2$ are calculated as follows:

$$\begin{cases} i < \frac{N}{2} \\ S1(i) = \max\left(i - \frac{1}{2}\left(2 + R_{DQ}(i)\right), 1\right) \\ S2(i) = S1(i) + R_{DQ}(i) + 2 \end{cases} \tag{4}$$

$$\begin{cases} i \geq \frac{N}{2} \\ S1(i) = \min\left(i - \frac{1}{2}\left(2 + R_{DQ}(i)\right), N - R_{DQ}(i) - 1\right) \\ S2(i) = S1(i) + R_{DQ}(i) + 2 \end{cases} \tag{5}$$

With such defined limits $S1$, $S2$ new formulations for weighting coefficients can be given:

$$\begin{cases} \omega_{i,j}^{(1)} = \frac{1}{x_j - x_i} \prod_{\substack{k=S1 \\ k \neq i,j}}^{S2} \frac{(x_i - x_k)}{(x_j - x_k)}, \quad j \in [S1, S2],\ i \neq j \\ \omega_{i,j}^{(1)} = 0, \quad j \notin [S1, S2] \\ \omega_{i,i}^{(1)} = -\sum_{k=S1}^{S2} \omega_{i,k}^{(1)} \end{cases} \tag{6}$$

and for the second order derivative:

$$\begin{cases} \omega_{i,j}^{(2)} = 2 \cdot \omega_{i,j}^{(1)} \cdot \left(\omega_{i,i}^{(1)} - \frac{1}{x_i - x_j} \right), & j \in [S1, S2], i \neq j \\ \omega_{i,j}^{(2)} = 0, & j \notin [S1, S2] \\ \omega_{i,i}^{(2)} = -\sum_{k=0}^{N} \omega_{i,k}^{(2)} \end{cases} \tag{7}$$

The key parameter of this method is rank distribution. Setting it correctly a very quick and accurate method can be obtained without the problems that appear during approximation with classic DQ method.

3. MATHEMATICAL MODEL

As an example of the RCDQ method application mathematical model for dendrite tip growth was chosen. The model was published by Żak *et al*. [4]. The computational domain is an interval on an axis that is the extension of the dendrite spherical envelope radius [R, $R_{\max}$]. The dendrite growth in metallic alloy can be described by a set of differential equations:

$$\begin{cases} \frac{\partial C}{\partial \tau} = D_S \left(\frac{\partial^2 C}{\partial r^2} + \frac{2}{r} \frac{\partial C}{\partial r} \right) \\ \left. \frac{\partial C}{\partial r} \right|_{r \to R} = -\frac{C_L - C_S}{D_S} \frac{dR}{d\tau} \\ \left. \frac{\partial C}{\partial r} \right|_{r = R_{\max}} = 0 \end{cases} \tag{8}$$

where: $C(r, \mathrm{t})$ [wt. %] denotes the function that describes the alloying element concentration in distance of r [m] from the dendrite centre, at time t [s]. R [m] is the dendrite spherical envelope radius, $R_{\max}$ [m] is the radius in infinity (such a big that no diffusion effect of solute depletion is noted), D_S [m^2 s^{-1}] is an alloying element diffusivity in melt. C_S [wt. %] is the concentration on the interface taken from the phase diagram for solidus line; C_L [wt. %] is the alloying element concentration on the interface taken from the phase diagram for the liquidus line.

The dendrite spherical envelope growth rate can be computed using the formula given by Burden and Hunt [15]:

$$\frac{dR}{d\tau} = \frac{D_S \Delta S_V}{8 \sigma_{sl} Q} (\Delta T_S)^2 \tag{9}$$

where σ_{sl} [Jm^{-2}] is the solid-liquid interfacial energy, Q [K] is the growth restriction factor [19], ΔT_S [K] is solutal undercooling, in order to simplify the model authors assumed that

$\Delta T_S = \Delta T = T_L - T(\tau)$. This assumption limits presented model to cases in which the Ti concentration near to dendrite tip is still low. The transient temperature in the analyzed element is approximated with an assumption of a constant cooling rate G [Ks^{-1}]. The temperature balance takes into account a fraction of already solidified volume:

$$\frac{\partial T}{\partial \tau} = G + \frac{\Delta H_V}{VC_{pV}} \frac{\partial V_S}{\partial \tau} \tag{10}$$

where ΔH_V denotes volumetric latent heat for aluminium (Tab. 1), $\frac{\partial V_S}{\partial \tau}$ is the rate of dendrite spherical envelope growth, $V = \frac{4}{3}\pi\left(R_{\max}\right)^3$.

A computational example was performed for aluminium, the impurities that exist in this material were represented with the additively rule [5] as titanium [19]. With this assumption the binary (Al-Ti) alloy was taken into account. The parameters that describe the process and material are gathered in Table 1.

Table 1. Physical parameters for the analyzed phenomenon

Quantity and units	Value
Ti content in alloy [wt. %] [19]	1.334
Entropy of fusion per unit volume, ΔS_V [J·K^{-1}·m^{-3}] [20]	1.112 10^6
Enthalpy of fusion per unit volume, ΔH_V [J·m^{-3}] [20]	9.5 10^8
Diffusivity of Ti in Al melt, D_S [m^2·s^{-1}] [21]	2.59 10^{-9}
Solid–liquid interfacial energy, σ_{sl} [J·m^{-2}][19]	0.158
Volumetric heat capacity of melt, C_{pV} [J·K^{-1}·m^{-3}] [21]	2.58 10^6
Cooling rate, G [K·s^{-1}]	3.5
Diameter of nucleation site on which the nucleation event took place, d [m]	10^{-6}
Equilibrium partition coefficient, k [22]	7
Tangent of liquidus slope, m_L [K (wt. %)$^{-1}$] [22]	25.63

There was no need for setting the initial temperature, as in the presented model only the solutal undercooling change is significant (Eq. 9). The process starts when the grain appears on the d diameter particle. It takes place when undercooling is larger or equal to ΔT_C. This is also a basis to calculate initial undercooling as curvature undercooling [19]:

$$\Delta T_C = \frac{4\sigma_{sl}}{\Delta S_V d} \tag{11}$$

The initial value for R is calculated as half of the particle diameter $R = \frac{d}{2}$. At the beginning of the process it is assumed that there is no Ti in the grain and that the Ti is equally distributed in the melt adjacent to the dendrite envelope. The Ti concentration in the melt is equal to its content in alloy. $R_{\max}$ was chosen to be $R_{\max} = 50d$.

4. NUMERICAL MODEL

The time domain is divided into equal intervals $\Delta\tau$. Time derivative is approximated using the explicit Euler's scheme. The RCDQ method was chosen to approximate the spatial derivatives in Eq. 8. Computations are divided into steps which approximate the concentration filed at moments $\tau_k = k\Delta\tau$ since the beginning of the process. At each time step the computational domain changes as its boundaries depends on R that changes according to Eq. 9:

$$S = \left\{ r_i : R(\tau) = r_1 < r_2 < \ldots < r_N = R_{\max} \right\} \tag{12}$$

The grid points are chosen according to following algorithm:

$$r_i = R + (i-1)\Delta r = R + (i-1)\left(\frac{R_{\max} - R}{N-1} \right) \tag{13}$$

The grid in each time step changes, but its points number remains the same. Concentration at former time step in r_i node is taken to be equal to this value at the point with i index.

The governing equation for the analyzed phenomenon after applying the RCDQ method can be rewritten as follows:

$$\begin{cases} C_1^{k+1} = -\dfrac{(C_L - C_S)\Delta S_V}{8\sigma_{sl} Q} \left(\Delta T(\tau_k)\right)^2 \left(\dfrac{\omega_{1,1}^{(2)}}{\omega_{1,1}^{(1)}} + \dfrac{2}{r_1} \right) - \dfrac{1}{\omega_{1,1}^{(1)}} \sum_{j=S1(1)}^{j=S2(1)} \omega_{1,j}^{(1)} C_j^k \\ C_2^{k+1} = C_2^k + D_S \Delta\tau \left(\sum_{j=S1(2)}^{j=S2(2)} \omega_{2,j}^{(2)} C_j^k + \dfrac{2}{r_2} \sum_{j=S1(2)}^{j=S2(2)} \omega_{2,j}^{(1)} C_j^k \right) \\ \vdots \\ C_{N-1}^{k+1} = C_{N-1}^k + D_S \Delta\tau \left(\sum_{j=S1(N-1)}^{j=S2(N-1)} \omega_{N-1,j}^{(2)} C_j^k + \dfrac{2}{r_{N-1}} \sum_{j=S1(N-1)}^{j=S2(N-1)} \omega_{N-1,j}^{(1)} C_j^k \right) \\ C_N^{k+1} = -\dfrac{1}{\omega_{N,N}^{(1)}} \sum_{j=S1(N)}^{j=S2(N)} \omega_{N,j}^{(1)} C_j^k . \end{cases} \tag{14}$$

5. RESULTS AND DISCUSSION

The computer software that realizes the algorithm given by Eq. 13 was created. During the computations a different number of grid points N = 30, 60, 90 was used. All used grids were uniformly distributed in the $[R(\tau), R_{\max}]$ domain. The time step during calculations was constant, $\Delta\tau = 10^{-6}$ s. The rank distribution function $R_{DQ}(i)$ was chosen as follows: two rank extreme values were chosen $Ra_{\min} = 5$, $Ra_{\max} = 15$. $R_{DQ}(i)$ in the grid boundaries is equal to the $Ra_{\min}$,

in neighbouring points rank is equal to $Ra_{\min}+1$, in adjoining points, that are closer to the domain centre rank grows by 2 per grid step until it reaches or exceed $Ra_{\max}$. If rank exceeded the $Ra_{\max}$ it is changed to be $Ra_{\max}$, this is the rank that is equal for all remaining points in the domain centre.

The results of computation, alloying element concentration after chosen time intervals since grain initiation, are shown in Figure 1. The application of the RCDQ method leads to a stable numeric scheme and the resulting curves have the desired shape and smoothness. Growing dendrite causes interface movement. This leads to enrichment surrounding melt with the alloying element, by the quantity that was pushed off by the growing dendrite. The presented graphs show the diffusion of Ti in Al range and gives us an idea about its rate. The concentration of the alloying element grows highly near to the dendrite tip. Diffusion rate is not so high in comparison with the grain growth rate as the concentration change is visible surrounding with a quite small radius. After 2 seconds it is larger than $1.2\cdot10^{-4}$ m and the grain radius is about $2.4\cdot10^{-5}$ m. The significant change of Ti concentration takes place on the range five times greater than the grain radius. This result is similar to the analysis mentioned by Greer *et al.* [19, 23].

The results of simulation in each case are very similar. It is clear that for denser grids curve is smoother, it is connected with the number of points presented in the graph. However, the values of the highest Ti concentration are similar. Also the diffusion range in all graphs is very close. This result suggests that it was not necessary to use a 90 points grid, as computation for a larger number of points consumes computer computational powers (more additions and multiplications).

The concentration of the Ti and Al after 2 s changes significantly near to the dendrite tip. Further computations according to above model are impossible because model parameters (Tab. 1) in enriched region are no longer true. New values of those parameters should be in use. Also the assumption of ΔT_S and $T_L - T(\tau)$ equality cannot be in use any more.

In the Figure 2 the curves of the Ti concentration distribution in the melt calculated for different grids are shown. However, the curves run through the similar values, the curve for the 30 points grid has higher values. The rank approximation in all cases is the same, but the grid step also affects the quality of the numerical solution. In the presented numerical model the difference can be caused by different Q factor values. When the alloying element content grows the grain growth rate drops. This feature is visible for loose grids.

In order to more precisely measure the computation error another analysis was made. The quantity of Ti that was pushed off by the growing grain was measured. On the other hand the quantity of this element in the melt was integrated. Those values were compared to the obtained error of the numerical solution:

$$\varepsilon = \frac{\left| 0.01334R(\tau) - \int_{R(\tau)}^{R_{\max}} \left(C(r) - 0.01334 \right) dr \right|}{0.01334R(\tau)} 100\% \tag{15}$$

To obtain the integral, that appears in formula Eq. 15, the numerical integration called the rectangle rule was used.

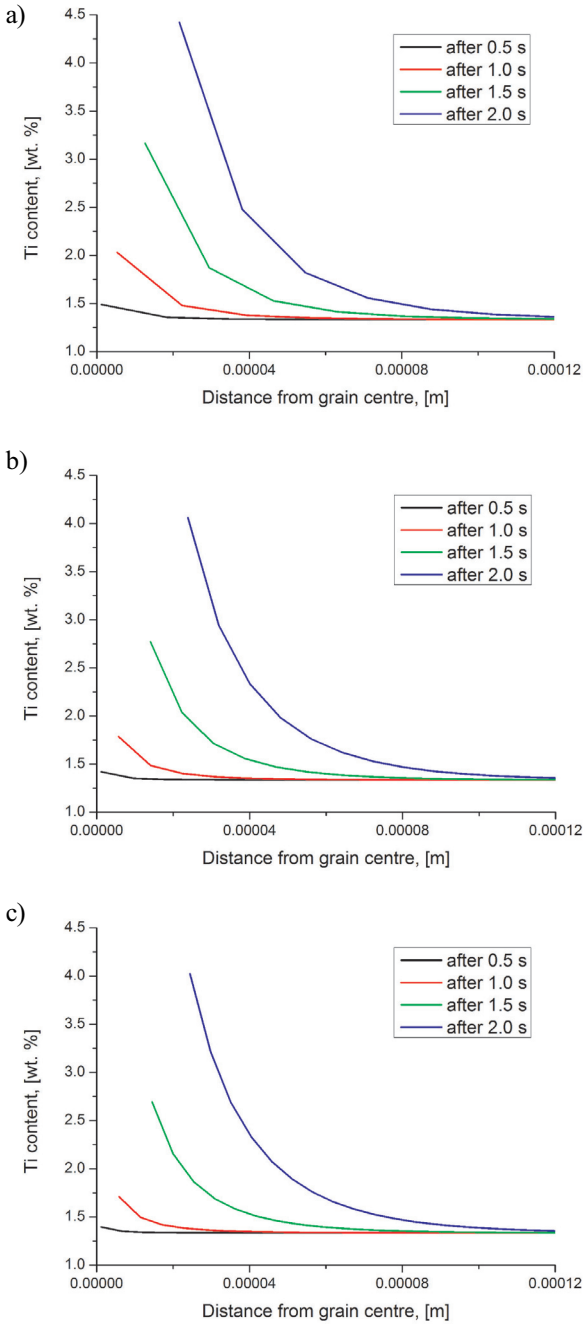

Fig. 1. *Ti concentration in liquid adjacent to the dendrite tip after 0.5, 1, 1.5, 2 seconds since grain initiation. Results of computations for grids of different density: a) 30 points; b) 60 points; c) 90 points*

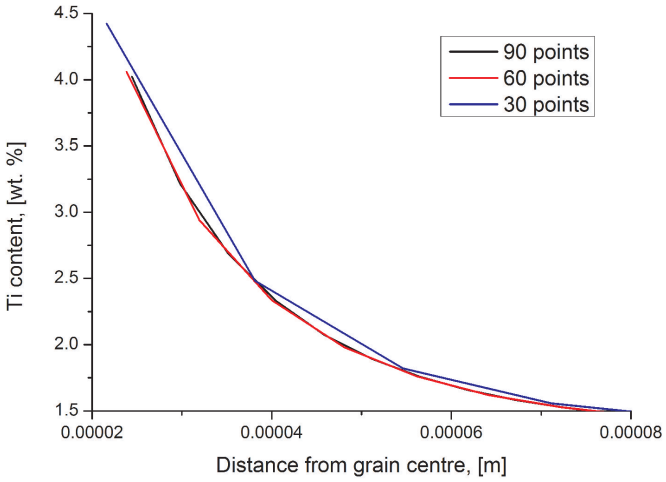

Fig. 2. *Comparison of Ti concentration distribution near to the dendrite tip. Results of computations after 2 s*

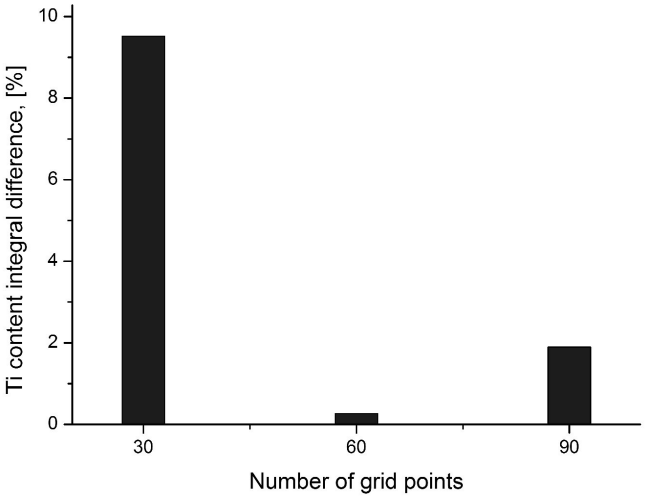

Fig. 3. *Percentage difference in the Ti content that was pushed off by the solid-liquid interface and its amount growth in the surrounding liquid. Results of computations after 2 s*

The percentage error is shown in Figure 3. It can be seen that the lowest error is for the 60 points grid. The error in this case is less than 0.3%. The results show that in all cases accuracy of computations is very high. The highest error is for the 30 points grid, but it is still lower than 10%. Such an error can be connected using the numerical integration method also, as it strongly depends on the grid step size. The loose grid has some features that can increase error. For instance in numerical modelling the average value in the grid point is taken

into account during calculations. This value represents all the adjacent region. If differences between the values in neighbouring points are large the approximation misses values that leads to an increase error (the value distribution usually is not linear).

6. CONCLUSIONS

The Rank Controlled Differential Quadrature method can be used to solve problems that are essential to Foundry Engineering.

Numerical approximation of partial derivatives with the RCDQ method produces very stable scheme for solving PDEs. This feature allows to solve even the moving grid problems with this method.

The growing grain changes the concentration of alloying elements in the melt. However, the length of this effect is not so large in comparison with the grain radius. The calculation shows that the concentration of those elements changes significantly near to the dendrite tip. High level of Ti near to the interface may cause a drastic change to the Q factor, that will significantly affect the dendrite growth rate.

Computations show that of the analyzed grids the optimal one is this with 60 points. In this case, the grid step was equal to $8.1 \cdot 10^{-6}$. The resulting curve was smooth and the accuracy measured with the Eq. 15 formula was very high in this case. It is also important not to increase $Ra_{\max}$ and grid density too much, as it costs computational effort.

Acknowledgements

The authors acknowledge financial support from the Ministry of Science and Higher Education under Dean's Grant AGH No. 15.11.170.424. A special thanks to Janusz Lelito and Beata Gracz for significant effort during this manuscript preparation.

REFERENCES

[1] *Piwowarski G., Krajewski W.K., Lelito J.*: Optimization of casting technology of the pressure die cast AZ91D Mg-based alloy, Metallurgy and Foundry Engineering, 36 (2010) 2, 105–111

[2] *Szucki M., Suchy J.S., Żak P., Lelito J., Gracz B.*: Extended free surface flow model based on the lattice Boltzman approach, Metallurgy and Foundry Engineering, 36 (2010) 2, 113–121

[3] *Gracz B., Lelito J., Krajewski W.K., Suchy J.S., Szucki M.*: Statistical analysis of SiC addition on heterogeneous nucleation of a-Mg primary phase in the AZ91/SiC composite, Metallurgy and Foundry Engineering, 36 (2010) 2, 123–130

[4] *Żak P.L., Lelito J., Krajewski W.K., Suchy J.S., Gracz B., Szucki M.*: Model of dendrite growth in metallic alloys, Metallurgy and Foundry Engineering, 36 (2010) 2, 131–135

[5] *Dahle A.K., Arnberg L.*: On the assumption of an additiveeffect of solute elements in dendrite growth, Materials Science and Engineering, A225 (1997), 38–46

[6] *Maxwell I., Hellawell A.*: A simple model for refinement during solidification, Acta Metallurgica, 23 (1975), 229–237

[7] *Rappaz M., Thevoz P.H.*: Solute diffusion model for equiaxed dendritic growth, Acta Materialia, 35 (1987), 1487–1497

[8] *Kapturkiewicz W., Fras E., Burbelko A.*: Computer simulation of the austenitizing process in cast iron with pearlitic matrix, Materials Science and Engineering A., 19 (2005), 1653–1659

[9] *Bellman R.E., Casti J.*: Differential quadrature and long-term integration, J. Math. Anal. Apply, 34 (1971), 235–238

[10] *Bellman R.E., Kashef B.G., Casti J.*: Differential quadrature: A Technique for the Rapid Solution of Nonlinear Partial Differential Equations, Journal of Computational Physics, 10 (1972), 40–52

[11] *Quan J.R., Chang C.T.*: New insights in solving distributed system equations by the quadrature methods – I, Comput. Chem. Engrg., 13 (1989), 779–788

[12] *Quan J.R., Chang C.T.*: New insights in solving distributed system equations by the quadrature methods – II, Comput. Chem. Engrg., 13 (1989), 1017–1024

[13] *Shu C., Chew Y.T.*: On the equivalence of generalized differential quadrature and highest order finite difference scheme, Computer methods in applied mechanics and engineering, 155 (1998), 249–260

[14] *Żak P.L.*: Differential Quadrature method application to computer simulation of heat transfer and solidification processes [in Polish], AGH Univesity of Science and Technology, Faculty of Foundry Engineering, Kraków (2012) PhD thesis [in press]

[15] *Vertesi P.*: Optimal Lebesgue constants for Lagrange interpolation, SIAM Journal on Numerical Analysis, 27 (1990), 1322–1331

[16] *Faber G.*: Über die interpolatorische Darstellung stetiger Funktionen, Jahresber der Deutschen Math., 23 (1914), 192–210

[17] *Żak P., Lelito J., Suchy J.S., Krajewski W.K.*: Improving the heat transfer numerical solution accuracy with application of Rank Controlled Differential Quadrature Method [Poprawa dokładności przybliżonego rozwiązania problemu transportu ciepła poprzez zastosowanie metody kwadratur różniczkowych sterowanego rzędu] (in Polish), Kraków: Komitet Metalurgii PAN, (2010), 278–285

[18] *Burden M.H., Hunt J.D.:* Cellular and dendritic growth II, Journal of Crystal Growth, 22 (1974), 109–116

[19] *Greer A.L., Bunn A.M., Tronche A., Evans P.V., Bristow D.J.*: Modelling of inaculation of metallic melts: Application to grain refinement of aluminium by Al-Ti-B, Acta Materialia, 48 (2000), 2823–2835

[20] *Brandes E.A. (ed.)*: Smithless Metals Reference Book, 6th edition. London: Butterworths, (1983)

[21] *Kurz W., Fisher D.*: Fundamentals of Solidification, 3rd edn. Laussane, Switzerland: Trans Tech. Publications, (1992)

[22] *Massalski T.B. (ed.)*: Binary Alloy Phase Diagrams, 2nd edn.: ASM International Materials Park, (1990)

[23] *Quested T.E., Greer A.L.*: Grain refinement of Al alloys: Mechanisms determining as-cast grain size in directional solidification, Acta Materialia, 53 (2005), 4643–4653

Received
February 2012